Influence of the Interfacial Zone on the Chloride Diffusivity of Mortars

A. Delagrave,* J.P. Bigas,† J.P. Ollivier,† J. Marchand,* and M. Pigeon*
*Concrete Canada and Centre de recherche interuniversitaire sur le béton (CRIB) Université Laval, Québec, Canada, G1K 7P4 and †Laboratoire Matériaux et Durabilité des Constructions, INSA-UPS Toulouse, France

Three different series of mortars with variable sand volume contents were cast in two different laboratories to study the influence of the interfacial transition zones (ITZ) on the transport coefficient of chloride ions. The first series was prepared and tested at Laboratoire Matériaux et Durabilité des Constructions (LMDC, Toulouse, France). The water/cement (w/c) ratio was 0.38 and the sand volume fractions were 0, 19, and 57%. The transport properties were investigated using a diffusion test. The two other series were prepared and tested at Centre de recherche interuniversitaire sur le béton (CRIB, Québec, Canada). The w/c ratios were 0.25 and 0.45 and the sand volume fractions were 0, 30, and 50%. The transport properties were assessed using a migration test. The test results indicate that aggregates modify the microstructure and the transport properties of mortars. The transport coefficient of chloride ions was found to decrease with an increase of the sand volume fraction. At the same time, the transport coefficient of the corresponding paste fraction was found to increase. The increased tortuosity of the matrix induced by the presence of aggregates thus appears to be more important than the influence of ITZ. The interconnection of ITZ was not found to lead to a rapid increase of the chloride ion transport coefficient. Advanced Cement Based Materials, 1997, 5, 86–92. *© 1997 Elsevier Science Ltd.*

KEY WORDS: Diffusivity, Migration, Microstructure, Cement Paste, Concrete, ITZ, Chlorides

The interfacial transition zone (ITZ) formed at the vicinity of aggregate particles in concrete is a very thin layer, typically 20–30 μm thick, of hydrated cement paste in which the microstructure differs significantly from that of the bulk volume. The ITZ is essentially characterized by a higher porosity and a gradient of the anhydrous and hydrated phases [1]. Numerous studies have indicated that the particular microstructural characteristics of the ITZ can be mainly attributed to the wall effect [1]; the aggregate particles disturbing the packing of cement grains at their vicinity. Modification of the ITZ microstructure can be achieved by changing the spatial arrangement of the small grains. This can be done by using a finer cement, a superplasticizer or silica fume [1–4]. An extensive description of the microstructure of the ITZ is beyond the scope of this paper and can be found in refs [1–4].

In recent years, the influence of the ITZ characteristics on the mechanical properties of concrete has been studied extensively. However, data on the effect of the ITZ on the durability of cement-based materials remain limited. From a theoretical point of view, the higher porosity of the ITZ should facilitate the ingress of external aggressive agents and favor the development of deleterious chemical reactions. Furthermore, the higher portlandite concentration usually found in the ITZ should also increase the potential risk of leaching caused by dissolution of $Ca(OH)_2$, and therefore detrimentally affects the resistance of concrete to ion penetration.

Given the inherent difficulties of calculating the volume and the properties of the ITZ in a sample, most investigations of the influence of paste/aggregate interface on transport properties have been made on model specimens where the complex and random structure of concrete is approximated by simpler geometries. Recent studies by Breton et al. [5] and by Bourdette [6] indicate that the effective diffusion coefficient of chloride ions is 6 to 12 times greater in the ITZ than in the bulk cement paste. Working with a twin geometrical model and assuming a 20-μm thickness of the ITZ, Ping et al. [7] have also calculated that the conductivity of the paste/aggregate interface should be 10 times greater than that of the bulk cement paste.

In concrete, the geometry of the pathways for the penetration of aggressive species is necessarily more complicated than in the simplistic models used by the previous authors. Recently, two complementary approaches have been introduced for evaluating the influence of ITZ on transport properties of concrete. Garboczi et al. [8,9] have developed a model to calculate the overall DC electrical conductivity of mortar. In this model, the mortar is described by a random arrangement of spherical sand grains surrounded by a 20-μm-thick ITZ. This model takes into account the difference in conductivity between the ITZ and the bulk cement

655 Avenue of the Americas, New York, NY 10010

ISSN 1065-7355/97/$17.00
PII S1065-7355(96)00008-9

paste. Using a similar approach, Bourdette et al. [6] studied the influence of the ITZ on the diffusivity of tritiated water in mortar samples. Results obtained by both models have clearly emphasized the fact that the concrete transport properties are influenced by the connectivity of ITZ and the excess in tortuosity introduced by increasing the aggregate content in the mixture. Results obtained by Garboczi et al. [9] have also underlined the importance of the ratio of conductivities C_{ITZ}/C_{paste} on the overall transport properties.

The present paper deals with the influence of the ITZ on the penetration of chloride ions in mortars. Two test series were conducted separately in two laboratories using different materials and experimental procedures. The results of the present investigation should help to better understand the mechanisms of chloride penetration in cement-based materials.

Test Program

Three different series of mixtures were cast. The first series was prepared and tested at LMDC (Toulouse, France), while the two remaining series were cast and tested at CRIB (Québec, Canada). Each series was made with a different type of cement. Each series was made of three different volume fractions of sand. Mercury intrusion porosimetry was used to study the pore structure of all mixtures. At LMDC, the influence of the interfacial transition zone on the chloride ion penetration was investigated using a diffusion test while at CRIB, the transport properties were assessed using a migration test.

Materials and Mixture Characteristics

Series 1: LMDC

The three mixtures prepared for this series had a fixed 0.38 water/cement (w/c) ratio and were made of a French OPC (CPA-CEM I 42.5) containing 3% limestone filler. The chemical analysis of this cement is given in Table 1. The sand volume fractions of each of the three mixtures were 0%, 19%, and 57%, respectively. The sand was a natural siliceous sand with a density of 2.65. The gradation curve is given in Figure 1 (Sand #1). To obtain a certain minimal workability, a naphthalene-based superplasticizer was added to the mortar mixture with a sand volume fraction of 57%. The admixture dosage was fixed at 1.2% of dry material by mass of cement. The composition of all mixtures is summarized in Table 2.

The specimens were cast in plastic molds (diameter = 11 cm, height = 22 cm). They were demolded after 1 day of moist curing and immersed immediately in a saturated lime solution for a 1-month period.

TABLE 1. Chemical and mineralogical compositions

Chemical analysis (%)	CPA CEM I	ASTM III	ASTM I
Silicon dioxide (SiO_2)	19.6	20.48	20.09
Aluminium oxide (Al_2O_3)	4.8	4.03	3.87
Ferric oxide (Fe_2O_3)	3.2	1.78	1.69
Calcium oxide (CaO)	64.1	64.73	63.82
Sulfur trioxide (SO_3)	3.3	3.33	3.50
Magnesium oxide (MgO)	0.9	2.31	2.22
Sodium oxide (Na_2O)	0.2	0.36	0.30
Potassium oxide (K_2O)	0.6	0.34	0.39
Titanium dioxide (TiO_2)	0.3	0.17	0.16
Manganese oxide (MnO)	0.1	0.05	0.05
Bogue Composition			
C_3S	64	68.7	68.7
C_2S	13	6.9	5.8
C_3A	8	7.7	7.4
C_4AF	11	5.4	5.1
Physical properties			
Blaine (cm^2/g)	2900	5351	4616
Specific density	3.1	-	-

- Data not available.

Series 2 and 3: CRIB

The two remaining series were prepared at CRIB. The w/c ratios of the two series were 0.25 and 0.45. The 0.25 w/c ratio mixtures were made of an ASTM Type III cement, and an ASTM Type I was used for the 0.45 w/c ratio mixtures. The chemical analyses of these two cements are included in Table 1.

The volume fractions of the sand in each series were 0%, 30%, and 50%, respectively. A standardized crushed siliceous sand having a density of 2.60 was used for all mixtures. The gradation curve is given in Figure 1 (Sand #2). For the 0.25 mixtures, a melamine-based superplasticizer was used at a dosage of 2.1% of dry material by mass of cement. The composition of all mixtures is summarized in Table 2.

All specimens were cast in plastic molds (diameter = 9.5 cm, height = 20 cm). The molds were sealed and

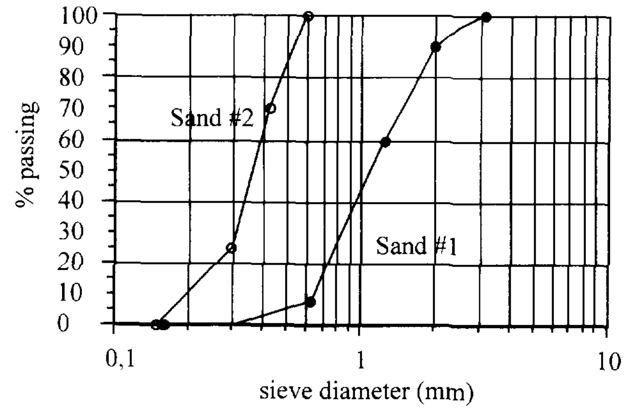

FIGURE 1. Granulometric distribution.

TABLE 2. Mixture compositions

Mixture	Cement	W/B	Sand volume (%)
M25-0	ASTM III	0.25	0
M25-30	ASTM III	0.25	30
M25-50	ASTM III	0.25	50
M38-0	CPA-CEM I	0.38	0
M38-19	CPA-CEM I	0.38	19
M38-57	CPA-CEM I	0.38	57
M45-0	ASTM I	0.45	0
M45-30	ASTM I	0.45	30
M45-50	ASTM I	0.45	50

rotated for the first 24 hours to prevent segregation. At the end of this period, the specimens were demolded and immersed in a saturated lime solution for 3 months.

Experimental Procedures

Series 1: LMDC

The chloride ion diffusivity of the three 0.38 w/c ratio mixtures was measured using a simple diffusion cell apparatus similar to the one described by Chatterji and Kawamura [10]. The test specimens (1-cm thick, 11-cm in diameter) were first immersed in a concentrated alkaline solution of KOH (4.65 g/l) and NaOH (1 g/l) and vacuum-saturated. The discs were then mounted on the diffusion cells. The upstream compartment of each cell was filled with the alkaline solution containing 20 g/l of chloride ions (NaCl). The same alkaline solution (KOH (4.65 g/l), NaOH (1 g/l)) was placed in the second compartment of each cell. Two duplicate specimens were tested for each mixture.

The chloride concentration of the solution in the downstream compartment was determined at regular intervals by means of potentiometric titration using a silver nitrate electrode. The experiments lasted approximatively 15 months. The effective chloride ion diffusion coefficient (*D*) was obtained from the steady-state regime according to Fick's first law:

$$J = -D\frac{\partial C}{\partial x} \tag{1}$$

where J represents the diffusive flux and $\partial C/\partial x$ the concentration gradient.

Because the main objective of this test series was to investigate the effect of ITZ on the transport properties of chloride ions, no corrections for the Nernst and Nernst-Planck retardations of ion mobility were made in the calculations of the chloride diffusion coefficient [11,12]. Although the values of *D* calculated according to eq 1 do not represent the "true" chloride ion diffusion coefficient (the value of *D* varies with the type and the concentration of the chloride solutions used in the experiment), it can be used on a comparative basis to study the influence of the mixture characteristics on the transport properties.

Samples for mercury intrusion porosimetry were vacuum dried before testing. All measurements were carried out using a Micromeritics apparatus. The instrument was capable of a minimum intruding pressure of 2.6 kPa and a maximum of 414 MPa. The contact angle assumed for all samples was 130°.

Series 2 and 3: CRIB

Discs 95-mm in diameter and 15-mm thick were used for the migration experiments. All the discs were immersed in deionized water and vacuum saturated for 24 hours before testing. The discs were then mounted on the migration cells for testing. The migration cells used in this study are similar to the one described by El-Belbol and Buenfeld [13]. Contrary to their experimental set-up, both compartments of the cells were equipped with an agitating device, and ruthenium-coated titanium electrodes were used. The upstream compartment of each cell was filled with a 0.3M (12 g/l) sodium hydroxyde solution containing 30 g/l of sodium chloride (0.5M). The downstream compartment of each cell was filled with a 0.3M (12 g/l) sodium hydroxyde solution.

A nominal voltage of 10 V was applied on each cell, and the temperature of the cells was kept constant at 23°C throughout the entire duration of the tests. The chloride concentration of the solution in the downstream compartment was determined at regular intervals by means of potentiometric titration using a silver nitrate electrode. The experiments lasted approximatively 3 weeks. The chloride ion migration coefficient (M) was obtained from the steady-state regime according to the following equation:

$$J = -D\frac{\partial C}{\partial x} + M\frac{zFE}{RT}C \tag{2}$$

where J represents the flux of chlorides migrating through the sample, *D* the chloride ion diffusion coefficient, $\partial C/\partial x$ the concentration gradient, *z* the ion valency (−1 in the case of chlorides), *F* the Faraday constant, *E* the external electrical field applied on the system, *R* the gas constant, *T* the temperature in Kelvin, and C the chloride concentration in the upstream compartment. For an applied voltage of 10 V, the total flux of chlorides passing through the sample is mainly driven by the electrical potential gradient, and the first term of eq 2 can therefore be neglected in the calculations.

To reduce the pore structure alteration induced by drying as much as possible, all samples for mercury porosimetry measurements were immersed in propan-2-ol for a minimal period of 21 days according to the procedure described by Feldman and Beaudoin [14]. At the end of this period, the samples were vacuum dried for 24 hours and tested. All measurements were carried out using a Micromeritics apparatus. The instrument was capable of a minimum intruding pressure of 2.6 kPa and a maximum of 207 MPa. The contact angle assumed for all samples was 130°. For each mixture, a minimum of two samples were tested.

Test Results

Mercury Intrusion Porosimetry

The porosimetry tests results for the three series are summarized in Table 3. The total porosities are presented in the second column of the table. The pore volume data was recalculated (on a unit volume of paste basis) considering that only the cement paste is porous. The results of these recalculations appear in the third column of the table.

The total porosity results show that the addition of sand generally tends to reduce the intrusion volume. As expected, the results also show that the total porosity increases with the w/c ratio. Table 3 shows that the porosity of the paste fraction appears to increase with the sand volume fraction, particularly for the mortars with a w/c ratio of 0.25. Bourdette et al. [6] and Winslow and Liu [15] have obtained similar results. They attributed this increase in the porosity that was available to mercury in the presence of numerous ITZ in the materials. At 0.25, the fraction of the total pore volume available to mercury is relatively low in neat pastes, but higher in mortars because of the change in the pore size distribution of the ITZ. In contrast, at a w/c ratio of 0.45, this phenomenon probably has little influence, as most of the pore volume of neat pastes is available to mercury.

TABLE 3. Porosity measurements

Mixture	Total Porosity (%)	Porosity paste fraction (%)
M25-0	8.5	8.5
M25-30	7.2	10.3
M25-50	8.0	16.0
M38-0	19.0	19.0
M38-19	20.0	25.0
M38-57	11.0	26.0
M45-0	21.9	21.9
M45-30	14.4	20.6
M45-50	12.0	24.0

Figure 2 presents the pore size distribution of the neat cement pastes for the 0.25 (Figure 2a) and 0.45 (Figure 2c) w/c ratio mixtures, whereas the porosity distribution for the 0.38 mixture is illustrated in Figure 2b. The pore size distribution of the paste fraction for the corresponding mortars with 50% (0.25 and 0.45 mixtures) and 57% (0.38 mixture) sand are also presented. For the 0.25 and 0.45 mixtures, the presence of aggregates tends to increase the volume of small pores without changing the overall distribution. For the 0.38 mixture, the addition of aggregates to a neat cement paste tends to coarsen the pore size distribution of the paste fraction by increasing the pore volume associated with a pore diameter ranging from 0.1 to 1μm. This can be explained, at least in part, to the shorter hydration period of the 0.38 mixtures.

Interfacial Transition Zone Interconnection

The degree of interconnection of the ITZ in each mixture was calculated using the model developed by Bourdette et al. [6] based on previous work done by Snyder et al. [16]. This model assimilates the mortar mixture to an arrangement of randomly distributed sand grains that are spherical in shape. The model also assumes that the ITZ surrounding the aggregate particles have a fixed thickness.

For the present study, various numerical simulations were run assuming in each case a different thickness of the ITZ. The results of these simulations are illustrated in Figure 3. It appears that, even for a 10-μ-thick ITZ, more than 95% of these interfaces are interconnected for a sand volume fraction of 50% (Sand #2) and for a sand volume fraction of 57% (Sand #1). This implies that for the sand volume fraction of 50% and 57% used, almost all the transition zones appear to be connected.

Diffusion and Migration Test Results

Table 4 presents the results of the diffusion measurements. The overall diffusion coefficient (Dm) of chloride ions appears to depend on the paste content of the mixtures. An increase of the sand volume fraction leads to a significant decrease of Dm. In this table, Dpm represents the diffusion coefficient recalculated on a unit volume of paste (considering no diffusion through the sand particles) and Dp is the diffusion coefficient of the neat paste (M38-0).

A similar trend can be observed in Table 5 where the migration test results are summarized. Mm represents the overall migration coefficient measured for the mortars whereas Mpm represents the migration coefficient recalculated on a unit volume of paste. Mp is the migration coefficient of the neat pastes (M25-0 and M45-0). For both w/c ratios, the chloride ion migration coefficient (Mm) decreases with an increase of the sand vol-

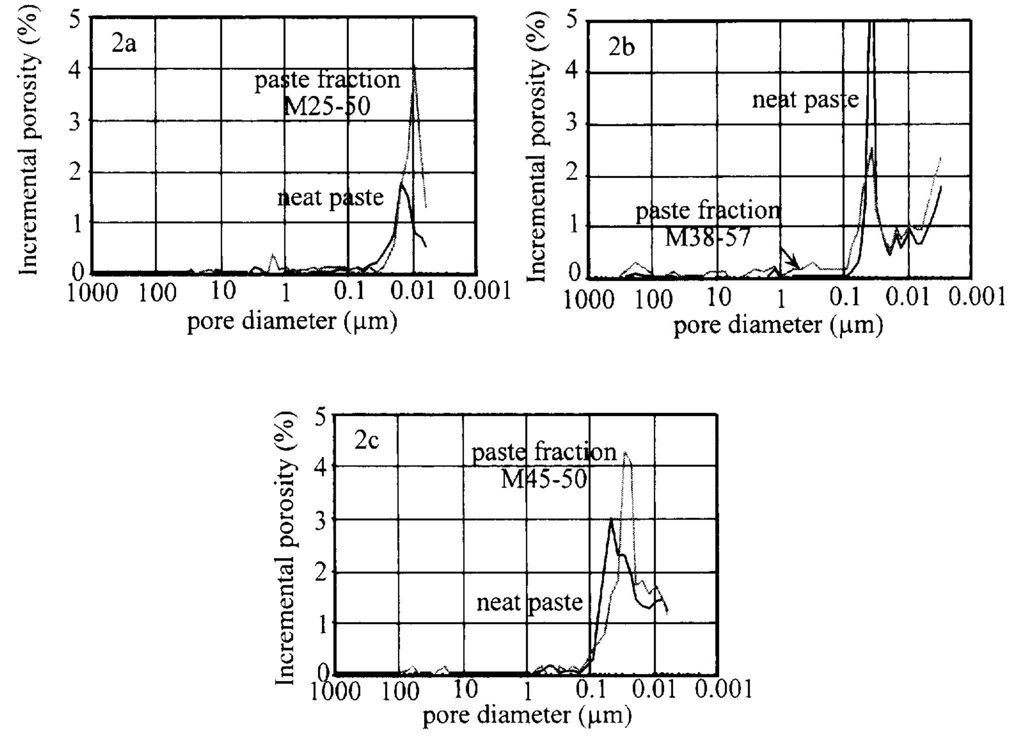

FIGURE 2. Pore size distribution for the neat cement pastes and the paste fraction of mortars 2a) M25-0 and M25-50, 2b) M38-0 and M38-57, 2c) M45-0 and M45-50.

ume fraction. Data in Table 5 also clearly indicate that the overall migration coefficient is directly affected by the w/c ratio. An increase of the w/c ratio from 0.25 to 0.45 has contributed to increase the migration coefficient by more than an order of magnitude.

The transport coefficients have been recalculated on a unit volume of paste basis. In these calculations, it was assumed that the aggregate particles act only as solid inclusions in the matrix. The recalculated values are given in Tables 4 and 5. They show that the transport properties of the paste fraction increase with the sand volume content of the mixtures. This increase can be attributed to the presence of the porous ITZ in the materials.

Discussion

The total porosity of the paste volume fraction of mortars measured in this investigation was found to increase with the sand volume fraction, particularly for the 0.25 mixtures. This increase in the porosity available to mercury can be attributed to the presence of numerous ITZ in the materials. As mentioned before, the ITZ tends to be more porous than the bulk cement paste.

The pore size distributions of the mixtures from series 1 (w/c = 0.38) are somewhat different from those of series 2 and 3 (w/c = 0.25 and 0.45). The results for series 2 and 3 show that the pore size distribution for the mortars and the neat cement pastes are quite simi-

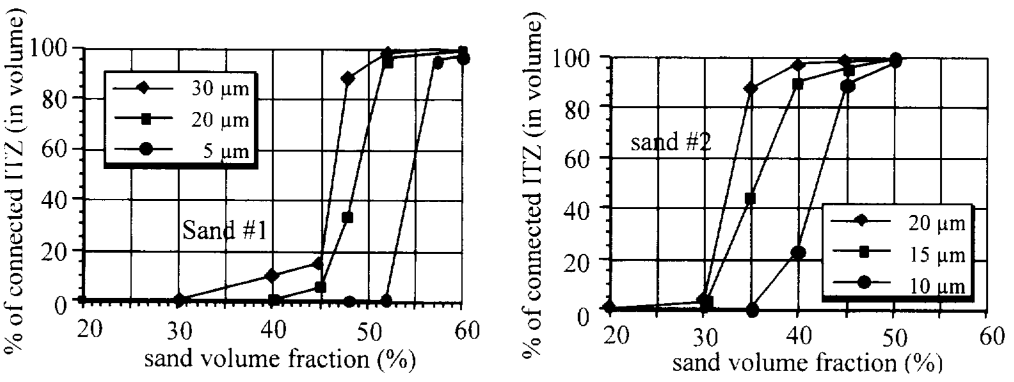

FIGURE 3. Connected fraction of ITZ in relation with the sand volume content.

TABLE 4. Diffusion coefficient of chloride ions

Mixture	Dm mortar ($10^{-12}m^2/s$)	Dpm paste fraction ($10^{-12}m^2/s$)	Dm/Dp
M38-0	0.89	0.89	1
M38-19	0.75	0.90	0.84
M38-57	0.56	1.33	0.63

lar, while the results for series 1 indicate that the pore size distribution for the mortar and the neat cement paste are different (see Figure 2). In this series, the results show a significant increase in the volume of pores between 0.1 to 1 μm when sand is added to the paste. At first glance, the results from series 2 and 3 appear to be in contradiction with previously published data that indicate an increase in the volume of large pores when sand is added to the paste [6,15]. It must be mentioned, however, that most of these porosity measurements were obtained on specimens cured only for a short time. Breton et al. [5] and Bourdette [6] have clearly shown that the porosity of ITZ decreases very quickly with the time of curing, because the new hydrates formed with time tend to fill the more open structure of the ITZ. The three month curing period for the series 2 and 3 specimens (as opposed to the shorter one month curing period for the series 1 specimens) can probably explain the lack of difference between the pore size distribution of the paste and the mortars. The preparation of the samples for the porosity measurements also differs between the two laboratories. At LMDC, the samples are vacuum-dried before mercury intrusion. This severe way of drying tends to open the pore structure of the ITZ which is more fragile. At CRIB, the samples were immersed in propan-2-ol before being vacuum-dried. The surface tension of the propan-2-ol is lower than that of the water which preserves the integrity of the microstructure [14].

Figure 4 presents the evolution of the mortar/neat paste transport coefficient ratio as a function of the sand volume fraction. For the sake of comparison, the conductivity (C) results obtained by Garboczi et al. [9] are also included in the figure. If the transport properties of the ITZ were similar to that of the bulk cement paste, the results would follow the $C_{ITZ}/C_{paste} = 1$ curve. The results of the diffusion and migration tests clearly show a linear decrease of the transport properties of mortars with the increase of the sand volume fraction. However, this reduction is not as large as it would be if the transport properties of the ITZ were the same as that of the bulk cement paste. In these calculations it is assumed that the microstructure of the matrix phase in mortar is the same as that of neat cement paste. This is probably not totally true. Because there is water conservation in the mortar, a higher water/binder ratio in the ITZ will result in a lower water/binder ratio in the bulk cement paste. This certainly affects the comparison between mortars and neat cement pastes because the volume of paste contained in the ITZ represents a significant volume of the total paste phase.

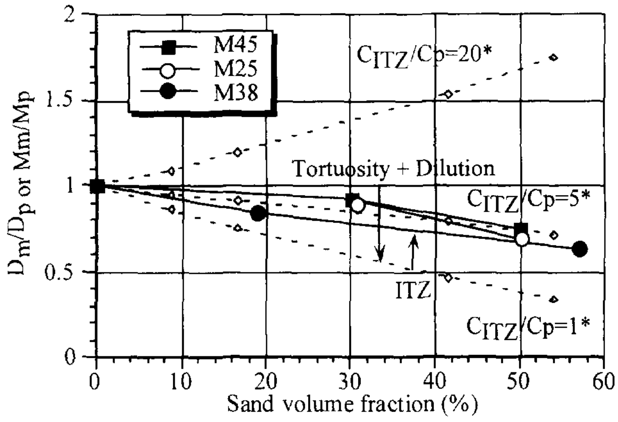

* From Garboczi [9]

FIGURE 4. Evolution of chloride ion diffusion in relation with the sand volume fraction.

TABLE 5. Migration coefficients of chloride ions

Mixture	Mm mortar ($10^{-12}m^2/s$)	Mpm paste fraction ($10^{-12}m^2/s$)	Mm/Mp
M25-0	0.18	0.18	1
M25-30	0.16	0.23	0.89
M25-50	0.10	0.20	0.56
M45-0	4.45	4.45	1
M45-30	3.58	5.11	0.80
M45-50	2.74	5.48	0.62

The presence of aggregates in a hydrated cement paste matrix has two opposite effects on the transport properties. First, the addition of solid particles leads to an increase in the tortuosity of the matrix. This implies that chloride ions have to move around the solid inclusions. Second, the presence of porous and connected ITZ probably contributes to facilitates the movement of ions. The overall transport properties of a given mortar sample will depend on the relative importance of these two opposite phenomena and on the ratio of transport properties of the ITZ to those of bulk cement paste. The transport properties of mortars tested in this investigation are influenced of these two opposite phenomena, and the test results show that the overall transport properties of the mortars were influenced more by the presence of aggregates than by the presence of ITZ.

As mentioned before, the mortar/neat paste transport coefficient ratio was found to decrease almost linearly with the increase of the sand volume fraction even though all the ITZ appear to be interconnected for 50% (0.25 and 0.45 mixtures) and 57% (0.38 mixture) of sand. The lack of a critical sand volume fraction with regard to the transport properties is in accordance with the results published by Hornain et al. [17] and by Garboczi et al. [9]. These results clearly indicate the fact that it is not the connectivity of ITZ that influences the transport properties but the ITZ/neat cement paste to transport properties ratio. The geometric fact of a percolation threshold would have been seen in the transport properties only if the phase being connected had a large transport coefficient compared to the matrix phase. According to Figure 4, the transport properties ratio between the ITZ and the neat cement paste is less than 5. It is thus not very surprising not to observe a sand volume threshold.

The linear decrease of transport properties of mortars for the 0.38 mixtures are somewhat surprising since the porosity measurements revealed a coarser pore size distribution with the presence of aggregates. However, it should be remembered that for the 0.38 mixtures, pore size distribution was measured after only 1 month of curing while the apparent diffusion coefficient was obtained after several months of test. The porosity of the ITZ evolved throughout the test. This underlines the importance of developing a rapid test procedure to investigate the influence of the ITZ on transport properties. The migration test appears to be an interesting tool to study this type of phenomenon. However, the short-term application of an electrical potential has been found to significantly modify the concrete microstructure [18,19]. Other investigations have indicated that the electrical potential may also modify the mechanisms of chloride interaction with hydrated cement pastes [20,21].

Conclusion

The presence of aggregates in cement paste tends to modify the microstructure and the transport properties of cementitious systems. The results presented show a global reduction of the chloride ion transport coefficient for mortars, but at the same time, there is an increase in the transport properties of the paste fraction because the porosity of the paste is modified by the presence of sand particles. This modification can be attributed to the presence of numerous interfacial transition zones. The presence of aggregates in cement pastes has two opposite effects on the transport properties. They act as solid inclusions increasing the tortuosity of the matrix while the presence of numerous ITZ tends to facilitate the movement of chloride ions.

The results presented did not indicate the existence of a sand volume threshold from which the overall transport coefficient increases rapidly. This clearly underlines that it is not the connectivity of ITZ that influences the transport properties but the ITZ/neat cement paste transport properties ratio. The test results also underline the need to develop a rapid test procedure to investigate the influence of the ITZ on the transport properties.

References

1. Ollivier, J.P.; Maso, J.C.; Bourdette, B. *Advn. Cem. Bas. Mat.* **1995,** *2,* 230–38.
2. Goldman, A.; Bentur, A. in *Interfaces in Cementitious Composites,* Maso, J.C. Ed., E.F. & Spon, London, **1992,** pp. 53–61.
3. Hanna, B. *Contribution to the study of the pore structure of mortars containing ultra-fine particules,* Ph.D. Thesis, INSA-Toulouse, France, **1992,** 177 p, (in French).
4. Scrivener, K.L.; Bentur, A.; Pratt, P.L. *Advn. Cem. Res.* **1988,** *1,* 230–237.
5. Breton, D.; Ollivier, J.P.; Ballivy, G. in *Interfaces in Cementitious Composites,* Maso, J.C. Ed., E.F. & Spon, London, **1992,** 279–288.
6. Bourdette, B., Ringot, E., Ollivier, J.P. *Cem. Concr. Res.* **1995,** *25,* 741–751.
7. Ping, W.; Beaudoin, J.J.; Brousseau, R. *Cem. Concr. Res.* **1991,** *21,* 515–522.
8. Garboczi, E.J.; Schwartz, L.M.; Bentz, D.P. *Advanced Cement-Based Materials* **1995,** *2,* 169–181.
9. Garboczi, E.J.; Schwartz, L.M.; Bentz, D.P. Bonding and Interfaces in Cementitious Materials, MRS symposium proceedings, **1994,** *370,* 429–436.
10. Chatterji, S.; Kawamura, M. *Cem. Concr. Res.* **1992,** *22,* 525–530.
11. Chatterji, S. *Cem. Concr. Res.* **1994,** *24,* 907–912.
12. Bockris, J.O.M.; Reddy, A.K.N. *Modern electrochemistry,* Plenum Press, New York, U.S.A., **1977,** 622 p.
13. El-Belbol, S.M.; Buenfeld, N.R. in *Pore Structure and Permeability of Cementitious Materials,* Roberts, L.R.; Skalny, J.P. Eds, Materials Research Society, 137, **1989,** 83–89.
14. Feldman, R.F.; Beaudoin, J.J. *Cem. Concr. Res.* **1991,** *21,* 297–308.
15. Winslow, D.; Liu, D. *Cem. Concr. Res.* **1990,** *20,* 227–235.
16. Snyder, K.A.; Winslow, D.N.; Bentz, D.P.; Garboczi, E.J. Advanced Cementitious Systems: Mechanisms and Properties, MRS Symposium proceedings, **1992,** *245,* 265–270.
17. Hornain, H.; Marchand, J.; Duhot, V.; Moranville-Regourd, *Cem. Concr. Res.* **1995,** *25,* 1667–1678.
18. Saito, H.; Nakane, S.; Ikari, S.; Fujiwara, A. *Nuclear Engineering Design* **1992,** *138,* 151–155.
19. Gérard, B. *Contribution des couplages mécanique-chimie-transfert dans la tenue à long terme des ouvrages de stockage de déchets radioactifs,* **Ph.D. Thesis,** Université Laval-École Normale Supérieure de Cachan, 293 p.
20. Tritthart, J.; Pettersson, K.; Sorensen, B. *Cem. Concr. Res.* **1993,** *23,* 1095–1104.
21. Enevoldsen, J.N.; Hansson, C.M.; Hope, B.B. *Cem. Concr. Res.* **1994,** *24,* 1525–1533.